Growth of Unidirectional Molecular Rows of Cysteine on Au(110)-(1 × 2) Driven by Adsorbate-Induced Surface Rearrangements

A. Kühnle,[1] L. M. Molina,[1] T. R. Linderoth,[1,*] B. Hammer,[1] and F. Besenbacher[1]

[1]*Interdisciplinary Nanoscience Center (iNANO), CAMP and Department of Physics and Astronomy, University of Aarhus, DK-8000 Aarhus C, Denmark*

(Received 12 May 2003; published 16 August 2004)

Using scanning tunneling microscopy we have studied the nucleation and growth of unidirectional molecular rows upon adsorption of the amino acid cysteine onto the anisotropic Au(110)-(1 × 2) surface under ultrahigh vacuum conditions. By modeling a large variety of possible molecular adsorption geometries using density-functional theory calculations, we find that in the optimum, lowest energy configuration, no significant intermolecular interactions exist along the growth direction. Instead the driving force for formation of the unidirectional molecular rows is an adsorbate-induced surface rearrangement, providing favorable adsorption sites for the molecules.

DOI: 10.1103/PhysRevLett.93.086101 PACS numbers: 68.43.Hn, 68.43.Bc, 81.07.Nb, 81.16.Dn

Self-assembly of supramolecular structures from organic molecules adsorbed on solid surfaces is interesting both for fundamental scientific reasons and because it is believed to be a promising route to formation of functional molecular architectures in the emerging area of nanotechnology. In general, molecular self-assembly at surfaces results from a subtle balance between molecule-molecule and molecule-surface interactions. Unidirectional molecular rows or "wires," for instance, in some cases self-assemble due to specific intermolecular interactions, such as head-to-tail hydrogen bonding or dipole-dipole coupling [1–3] while the orientation of such structures along high-symmetry directions on the surface reflects weaker molecule-surface interactions. In other cases molecule-surface interactions dominate, directing unidirectional molecular growth along preexisting templates on the surface such as step edges [4–6] or atomic rows [7]. If the adsorbate-surface interaction is sufficiently strong, adsorption induced surface rearrangements can occur. While this is a well-known phenomenon for atomic adsorbates [8], it is relatively unexplored in the context of self-assembly of organic molecules on surfaces [9–11].

In this Letter we investigate adsorption structures formed from the naturally occurring amino acid cysteine [HS-CH_2-CH(NH_2)-COOH] on the missing-row reconstructed Au(110)-(1 × 2) surface. Through an interplay between scanning tunneling microscopy (STM) measurements and density-functional theory (DFT) calculations we find that the cysteine molecules self-assemble into molecular rows, not because of significant intermolecular interactions along the row direction, but because the molecules preferentially adsorb in unidirectional trenches created by the removal of atoms from the close-packed gold rows of the missing-row reconstructed surface. Formation of extended molecular rows, as opposed to individually adsorbed or clustered molecules, minimize the energy cost associated with this surface rearrangement, providing an effective intermolecular attraction which acts as the driving force for the molecular self-assembly.

For the presently studied model system, the self-assembly of surface-bound organic molecules is thus dominated by a dynamic response of the surface to the molecular adsorption [12], rather than specific intermolecular interactions or a simple surface template effect. The present account is the first detailed and quantitative investigation of such a molecular self-assembly system where the energetics of adsorbate-induced surface rearrangement determines broad features of a molecular assembly pattern and dominates over direct intermolecular interactions.

The experiments were performed in an ultrahigh vacuum chamber equipped with the homebuilt Aarhus STM [8,13]. The gold crystal was cleaned by repeated cycles of Ar ion sputtering at 1.5 keV and annealing at 800 K, resulting in a well-ordered Au(110)-(1 × 2) surface [14]. The enantiomerically pure D or L cysteine molecules were vapor deposited from a glass crucible heated to approximately 360 K. The structures discussed below form upon evaporation of submonolayer coverages of cysteine onto a gold surface held at room temperature, followed by annealing at 380 K for about 15 min (STM imaging was performed at room temperature).

An STM image giving an overview of the surface after adsorption of D cysteine molecules is shown in Fig. 1. The close-packed rows of gold atoms characteristic of the missing-row reconstructed surface appear as stripes running vertically in the image along the $[1\bar{1}0]$ direction (see the ball model in Fig. 2(e)]. Two coexisting cysteine structures are observed: (i) extended unidirectional molecular double rows running along the $[1\bar{1}0]$ direction (marked 1) and (ii) randomly distributed molecular double lobe features (marked 2). The latter structure has been discussed in detail elsewhere [15] and consists of cysteine dimers linked by double hydrogen bonds be-

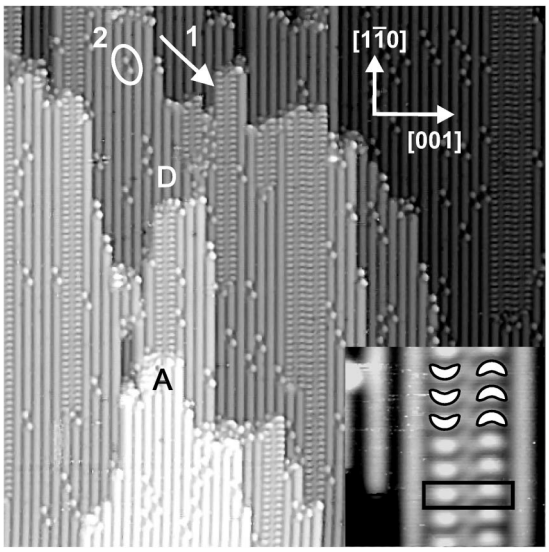

FIG. 1. Large-scale STM image showing coexisting molecular structures of D cysteine on a Au(110)-(1 × 2) surface (425 × 425 Å, constant-current mode $I = -0.1$ nA, $V = -1.2$ V applied at the sample). The molecular double-row structure (1) is terminated at ascending (A) or descending (D) step edges or at defects on the terraces. Inset: a close-up of a double-row formed from D cysteine molecules (40 × 40 Å). The unit cell of this structure is depicted in black.

tween carboxylic groups and adsorbed on a four-atom long vacancy in the close-packed gold rows. Here we focus on the molecular double rows (1), consisting of "bean-shaped" entities stacked into rows along the [1$\bar{1}$0] direction and paired in the [001] direction to the observed double rows. (Isolated individual rows are not observed.) The separation between the two rows within a double row is ~10 Å in the [001] direction and the periodicity along the [1$\bar{1}$0] direction is 5.8 Å (twice the Au-Au lattice distance). These dimensions suggest that each bean-shaped entity in the rows corresponds to one cysteine molecule.

The cysteine rows protrude in the STM images by only 0.16 Å relative to the gold atoms in the close-packed Au rows. This should be compared with the 0.6 Å protrusion of the individual cysteine dimers (2) which are bound to a vacancy structure in the close-packed gold rows of the Au(110)-(1 × 2) surface [15]. It therefore appears unlikely that the cysteine molecular rows are adsorbed on top of close-packed Au rows of the uppermost (1 × 2) surface layer. Instead we propose that the adsorption of the cysteine molecules induces a surface rearrangement where atoms in two adjacent close-packed Au rows are removed, allowing the unidirectional cysteine double-row structures to be adsorbed on patches of unreconstructed Au(110)-(1 × 2) surface.

The absence of mirror symmetry in the double-row structure (e.g., the opposite orientation of the bean-shaped objects in adjacent rows as indicated by exaggerated white symbols in the inset of Fig. 1) is a reflection of the chirality of the cysteine molecule. Evaporation of the other enantiomer, L cysteine, indeed results in a similar, but mirror-imaged, asymmetric double-row structure. Since the molecules thus retain their chirality within the double-row structure, they cannot be fragmented to any significant degree.

On large terraces, the cysteine double rows extend over several hundreds of angstroms. Out of 138 double rows 50% have both ends at step edges, 49% have one end at a terrace and the other at a *descending* step edge, while only 1% have one end at a terrace and the other at an *ascending* step edge (see Fig. 1). No rows are observed with both ends on a terrace. If nucleation of the double rows occurred on the terraces, an equal number of rows should end at descending and ascending step edges for symmetry reasons, and one would expect rows with both ends on a terrace. We therefore conclude that descending step edges constitute the nucleation sites of the double rows, which grow until they reach an ascending step edge or are otherwise terminated.

To complement the experimental findings, we have performed state-of-the-art DFT calculations for a large variety of possible cysteine adsorption configurations on both the bulk-truncated Au(110)-(1 × 2) surface and the missing-row reconstructed Au(110)-(1 × 2) surface (see Fig. 2). The calculations were carried out using the DACAPO code with a plane wave basis set ($E_{\mathrm{cut}} =$ 25 Ry), ultrasoft pseudopotentials, and the PW91 XC functional [16]. The Au(110) surface was modeled using a slab geometry of three layers. The two lower Au layers were kept fixed whereas the remaining Au atoms and all atoms within the cysteine molecules were fully relaxed until the total sum of residual forces was below 0.5 eV/Å (corresponding to ~0.01 eV/Å per atom or equilibrium structures converged with an accuracy well below 0.05 eV per unit cell). Calculations with five gold layers confirm that the adsorption energies obtained for three layers have a precision of 0.1 eV per unit cell.

Cysteine, like other thiols [17], becomes bound to gold surfaces via dehydrogenation of the mercapto (-SH) group resulting in the formation of a fairly strong (1.5–2.5 eV [18]) covalent S-Au bond [19,20]. Therefore one (dehydrogenated) cysteine molecule was introduced per bean-shaped entity in Fig. 1. To conform with the STM findings only structures with C_2 symmetry were considered and the calculations were performed in a (2 × 5) surface unit cell containing two cysteine molecules. The lowest energy adsorption configuration identified, shown in Fig. 2(b), was found on the unreconstructed Au(110)-(1 × 2) surface [Fig. 2(a)]. The unreconstructed surface is higher in energy than the reconstructed one by 0.10 eV per (1 × 2) unit cell implying that the cysteine-induced rearrangement of the topmost Au layer costs 0.40 eV for each double-row repeat unit [see also Figs. 4(a) and 4(b)]. In the lowest energy adsorption configuration, Fig. 2(b), the cysteine molecules pair as

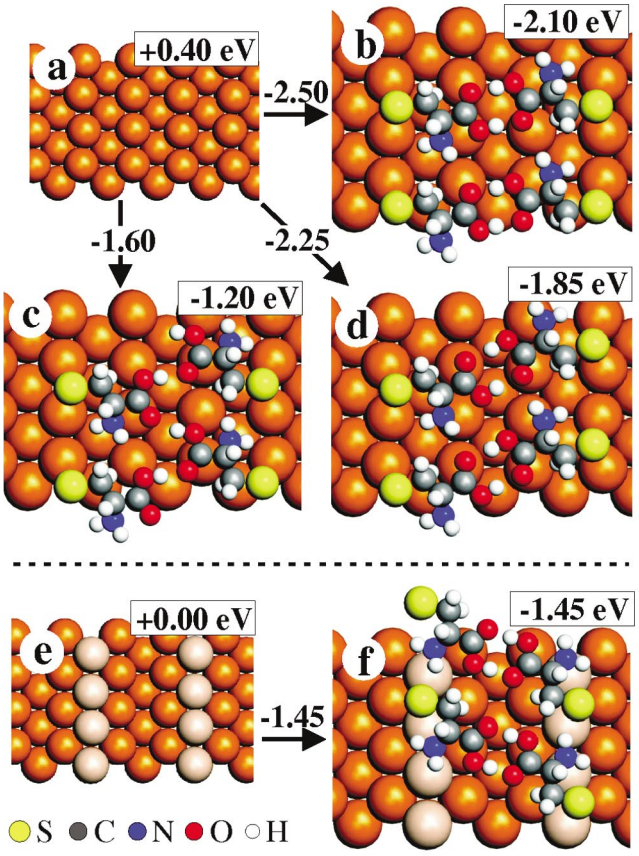

FIG. 2 (color). Selected adsorption structures considered in DFT calculations. (a) Bulk-truncated Au(110)-(1 × 1) surface. (b) The most stable D cysteine double-row structure identified. (c) "Zigzag" structure where each molecule forms hydrogen bonds with two molecules in the adjacent row. (d) A similar structure as in (b), but with the S adsorption site on one row shifted along $[1\bar{1}0]$. (e) Missing-row reconstructed Au(110)-(1 × 2) surface. (f) Optimum structure identified on the Au(110)-(1 × 2) surface. The arrows indicate the energy balance for the reaction Au(110) + 2cysteine → H_2 + 2cysteinate/Au(110). For (b)–(d), the final formation energies (shown in the upper right corners of the models) are obtained by adding the 0.40 eV required to lift the missing-row reconstruction.

dimers by OH-O hydrogen bonds between carboxylic groups while the molecules are anchored to the gold surface by S-Au bonds and by weaker bonds between the lone pair of the amino groups and surface gold atoms. The cysteine dimers are packed along $[1\bar{1}0]$, but there are no direct intermolecular bonds in this direction.

The formation of unidirectional molecular rows intuitively suggests a strong intermolecular interaction along the growth direction. The high resolution STM image in the inset in Fig. 1 also indicates an interconnecting zigzag structure within the double row. We therefore considered the structure shown in Fig. 2(c), where the carboxylic group forms hydrogen bonds to two molecules in the opposite row, providing a net interconnection along the row direction. However, this structure is higher in energy, compared to the one in Fig. 2(b), due to stretching of the gold-nitrogen bonds from 2.4 to 2.9 Å. A number of other structures with interconnecting hydrogen bonds in the direction of the double row, including one with hydrogen bonds between carboxylic and amino groups as a precursor of a peptide bond formation, were also less stable than the model in Fig. 2(b).

A configuration where the S-Au binding site for one of two opposite cysteine units is shifted by half a repeat distance is shown in Fig. 2(d) (inspired by the shift in the position of the bean-shaped entities in opposite rows apparent from the inset in Fig. 1). However, this structure can be realized only by stretching the OH-O bonds from 1.6 to 1.7 Å, resulting again in a higher energy structure.

We have in Fig. 3 superimposed the lowest energy configuration of the cysteine double rows, Fig. 2(b), on an STM image to allow comparison with the experimental findings. This structure is preferred due to its combination of optimum bond lengths and the coordination of each surface Au atom to no more than one cysteine functional group at a time. The lowest energy molecular configuration identified on the reconstructed Au(110)-(1 × 2) surface [Fig. 2(f)] is less stable since on this surface some gold atoms must bind to both the sulfur and the nitrogen atom on one cysteine molecule.

In the gas phase, two cysteine molecules interact most strongly by forming double hydrogen bonds between their carboxylic groups, as shown by DFT calculations [15]. Chain formation on the surface cannot result from this preferential interaction, however. Instead it causes dimerization as observed for the isolated cysteine pairs [15] and the cysteine double rows (the absence of isolated, individual rows supports this conclusion). Without covalent or hydrogen chemical bonding between the repeat units of the double rows, we have to look elsewhere to identify the driving force for the formation of extended molecular rows. The direct interaction energy between two neighboring repeat units originating from static van der Waals (vdW) forces, such as dipole-dipole inter-

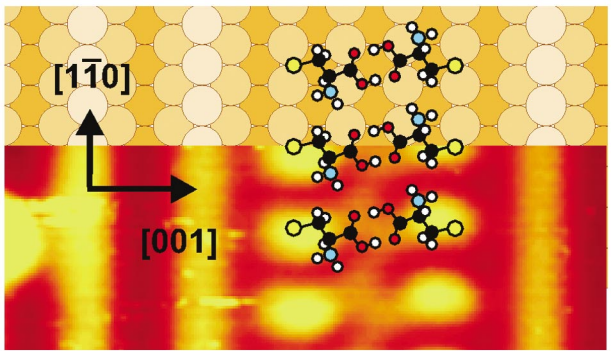

FIG. 3 (color). Most stable cysteine double-row structure, as obtained from the DFT calculations, superimposed onto an STM image. Note that also adjacent double rows, as observed occasionally in Fig. 1, are consistent with this model.

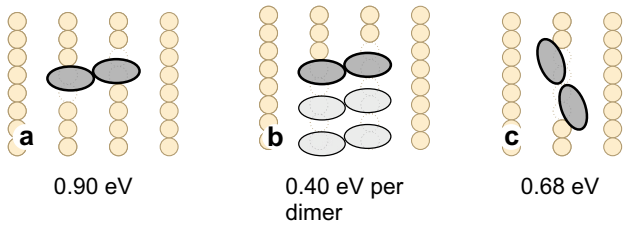

FIG. 4 (color online). Gold vacancy formation energies: (a) 0.90 eV for initiating a double row on the terrace, (b) 0.40 eV for continuing the growth of a cysteine double row, and (c) 0.68 eV for creating a four Au atom vacancy site for the isolated cysteine dimer of Ref. [15]. These energies result from appropriate summations of the energy costs of 0.31, 0.14, 0.12, and 0.11 eV for the removal of the first through fourth gold atom, respectively, in a close-packed gold row [obtained from DFT calculations in a (6×1) surface unit cell].

actions, is estimated to be 0.15 eV from DFT calculations examining energy versus separation for two repeat units (each containing two molecules) frozen in the optimum configuration of Fig. 2(b), but removed from the gold substrate. (The DFT approach neglects dynamical contributions to the vdW interactions [21], but these are believed to be insignificant in the present case.)

This direct molecule-molecule interaction is, however, dominated by an effective attraction resulting from the molecule induced surface rearrangement. For each repeat unit of the double rows, four Au atoms are removed in two adjacent Au rows [see Figs. 4(a) and 4(b)]. The cost of nucleating a four-atom vacancy to contain the first double-row repeat unit [Fig. 4(a)] is 0.90 eV, while it is only 0.40 eV for expanding a double row already formed [Fig. 4(b)]. The difference arises because the removal of the first and the second Au atom from an unbroken close-packed Au row is more energy demanding (0.31 and 0.14 eV, respectively) than the removal of the nth Au atom in a row (0.10 eV). This is because the removal of the first Au atom, besides from lifting the reconstruction locally, introduces two Au kink atoms in the row, as opposed to the removal of subsequent Au atoms that move these existing kinks only further apart. In effect, there is thus a net energy gain in the surface rearrangement energy of 0.50 eV associated with the (hypothetical) process of attaching an isolated repeat unit situated in a four-atom vacancy [Fig. 4(a)] to a molecular row [Fig. 4(b)].

Although the calculated energies required to lift the (1×2) reconstruction are not attributable as energy barriers, Fig. 4 nevertheless suggests that two cysteine molecules must overcome a much larger barrier for creating a nucleation site of a new double row than for continuing the growth of an already existing double row. This explains why, in the experiment, the descending step edge is found to be the only active nucleation site, since, at this edge, the gold kink sites already exist, reducing the cost for nucleating the double-row structure.

In summary, we have investigated how rearrangement of surface atoms induced by molecular adsorption may act to provide an effective attraction driving the formation of unidirectional, self-assembled molecular-row-type nanostructures, even when direct adsorbate-adsorbate bonding along the growth direction is insignificant. Fundamental insights into supramolecular self-assembly on surfaces are crucial in order to be able to devise strategies for the creation of functional molecular nanoarchitectures, and the mechanism studied here may be a route for nanostructuring of surfaces applicable to other systems. The results are also interesting from the perspective that adsorption and ordering of small biomolecules on solid surfaces is speculated to have played a role in early formation of biological macromolecules [22].

This work was supported by the Danish National Research Foundation, by The Danish Natural Science Research Council, and by the Danish Center for Scientific Computing.

*Electronic addresses: trolle@phys.au.dk
www.phys.au.dk/camp/

[1] J.V. Barth *et al.*, Angew. Chem., Int. Ed. Engl. **39**, 1230 (2000).
[2] T. Yokoyama *et al.*, Nature (London) **413**, 619 (2001).
[3] M. Böhringer *et al.*, Phys. Rev. Lett. **83**, 324 (1999).
[4] G. Koller, S. Surnev, F. P. Netzer, and M. G. Ramsey, Surf. Sci. **504**, 11 (2002).
[5] P.W. Murray, I. M. Brookes, S. A. Haycock, and G. Thornton, Phys. Rev. Lett. **80**, 988 (1998).
[6] M. T. Cuberes, R. R. Schlittler, and J. K. Gimzewski, Appl. Phys. Lett. **69**, 3016 (1996).
[7] G. Lopinski, D. Wayner, and R. Wolkow, Nature (London) **406**, 48 (2000).
[8] F. Besenbacher, Rep. Prog. Phys. **59**, 1737 (1996).
[9] M. Schunack *et al.*, Phys. Rev. Lett. **86**, 456 (2001).
[10] F. Rosei *et al.*, Science **296**, 328 (2002).
[11] X. Zhao, J. Am. Chem. Soc. **122**, 12584 (2000).
[12] S. Lukas, G. Witte, and C. Wöll, Phys. Rev. Lett. **88**, 028301 (2002).
[13] E. Lægsgaard, F. Besenbacher, K. Mortensen, and I. Stensgaard, J. Microsc. **152**, 663 (1988).
[14] T. Gritsch, D. Coulman, R. J. Behm, and G. Ertl, Surf. Sci. **257**, 297 (1991).
[15] A. Kühnle, T. R. Linderoth, B. Hammer, and F. Besenbacher, Nature (London) **415**, 891 (2002).
[16] J. P. Perdew *et al.*, Phys. Rev. B **46**, 6671 (1992).
[17] F. Schreiber, Prog. Surf. Sci. **65**, 151 (2000).
[18] L. M. Molina and B. Hammer, Chem. Phys. Lett. **360**, 264 (2002).
[19] Z. Sljivancanin, K.V. Gothelf, and B. Hammer, J. Am. Chem. Soc. **124**, 14 789 (2002).
[20] R. Felice, A. Selloni, and E. Molinari, J. Phys. Chem. B **107**, 1151 (2003).
[21] E. Hult, P. Hyldgaard, J. Rossmeisl, and B. I. Lundqvist, Phys. Rev. B **64**, 195414 (2001).
[22] B. M. Rode, Peptides **20**, 773 (1999).